Oral Presentation

The 7th TSME International Conference on Mechanical Engineering
13-16 December 2016

CST0007

# Behavior of Impurity in ITER using BALDUR code

Y. Onsa[1,*], W. Buangam[1], A. Wisitsorasak[2], B. Somjinda[1], and T. Onjun[1]

[1]School of Manufacturing Systems and Mechanical Engineering, Sirindhorn International Institute of Technology, Thammasat University, Klongluang, Pathumthani, Thailand
[2]King Mongkut's University of Technology Thonburi, Bangkok, Thailand
[*] Corresponding Author: E-mail: yutonsa_aero@yahoo.com, Phone: +6691-798-9009

***Abstract***

In this work, the behaviors of impurity in ITER plasma are predicted using the BALDUR code, which is used to carry out an evolution of plasma current, densities and temperature of ITER in type I ELMy H-mode scenarios. In these simulation, the plasma core transport that including ion and electron thermal, hydrogenic and impurity transport, are predicted using a linear combination of anomalous and neoclassical transports. An anomalous transport is calculated using a theory based Multimode (MMM95) model; while the neoclassical transport is calculated using NCLASS model. The temperature and density at the boundary are prescribed. Six species of impurity, including Lithium, Beryllium, Carbon, Nitrogen, Oxygen, and Neon, are considered. The fusion power degradation is observed with the increase of impurity atomic mass, in which mainly due to the increase of plasma radiation loss.

***Keywords****:* Plasma; Modeling; ITER; Impurity

## 1. Introduction

The presence of impurity in nuclear fusion reactor is considered one of the concerned issues because impurity can radiate energy and dilute fuel, which can strongly affects the performance of nuclear fusion in International Thermonuclear Experimental Reactor (ITER) which is built to demonstrate the scientific and technological feasibilities of a fusion power plant. Helium ash (alpha particle) is inevitable in fusion reactors because it is a product of deuterium-tritium (D-T) nuclear fusion reaction. Beryllium (Be), carbon (C) and oxygen (O) are also considered impurity which can be released from plasma facing components [1], [2], [3]. In addition, plasma facing components made of lithium can reduce the flux of recycled particles entering the plasma edge from the plasma facing components [4]. Unlike other impurities, nitrogen (N) and neon (Ne) are extrinsic impurity. The work of Schweinzer et al. [5] shows that an injection of nitrogen can reduce the thermal load on the diverter by radiating the power to the main chamber, while the work of Beurskens et al. [6] shows that an appropriate injection of neon can reduce the ELM energy loss. As a result, it is crucial to investigate these impurities behavior in ITER, especially the impurity transport and accumulation, which can lead to a way to improve the ITER performance. The accumulation of these impurities can cause many problems such as core radiation enhancement, fuel dilution or even plasma disruptions [6]. The predictive density at the boundary is fixed model by W.Buangam [7].

In this work, the behaviors of impurity on impurity transport and accumulation in ITER are studied by using 1.5D BALDUR integrated predictive modeling code. Predictive density boundary is used. This paper is organized as follows: brief descriptions of relevant components of the BALDUR code, including the Multimode Core Transport Model (MMM95) and NCLASS Module given in section 2; the prediction of ITER plasma profiles are presented and discussed in section 3; and summary is given in section 4.

## 2. BALDUR integrated predictive modeling code

The BALDUR integrated predictive modeling code [8] has been used intensively and widely to calculate the time evolution of various tokamak plasma properties, including electron and ion temperatures, deuterium and tritium densities, helium and impurity densities. The BALDUR code self consistently computes these profiles by mixing many physical processes together in the form of modules including transport, plasma heating, particle flux, boundary conditions and etc. It was found that the BALDUR code could yield results in a very good agreement with experimental data. For example, in [9-10], the BALDUR simulations with the MMM95 transport model yielded an agreement of about 10% relative root mean square (RMS) deviation.

### 2.1 Multimode Core Transport Model (MMM95

The Multi-Mode Model version 1995 (MMM95) [11] is a combination of theory-based transport models used to predict plasma profiles in tokamaks. It consists of the Weiland model for the ion temperature gradient (ITG) and trapped electron modes (TEM), the Guzdar–Drake model for drift-resistive ballooning modes, and kinetic ballooning modes. Usually, the Weiland model

for drift modes provides the largest contribution, followed by the drift- resistive ballooning mode and the kinetic ballooning mode respectively. The expressions of transport coefficients in MMM95 are:

$$\chi_i = 0.8\chi_{i,ITG\&TEM} + \chi_{i,RB} + 0.65\chi_{i,KB}$$

$$\chi_e = 0.8\chi_{e,ITG\&TEM} + \chi_{e,RB} + 0.65\chi_{e,KB}$$

$$D_H = 0.8D_{H,ITG\&TEM} + D_{H,RB} + D_{H,KB}$$

$$D_Z = 0.8D_{Z,ITG\&TEM} + D_{Z,RB} + D_{Z,KB}$$

**2.2 NCLASS Module**

The NCLASS module [12] calculates the neoclassical transport properties of multi-species axisymmetric plasma of arbitrary aspect ratio, geometry and collisionality. The neoclassical effects refer to the flows of Coulomb collisions between particles drifting in nonuniform magnetic and electric fields. This module determines a multifluid model for the parallel and radial force balance equations from which the neoclassical bootstrap current, parallel electrical resistivity, impurity and fuel ion radial particle transport, ion radial thermal transport and plasma poloidal rotation. It is designed to be called from a transport code that provides the plasma density and temperature profiles.

**2.3 Pedestal density model**

The experimental line average density and pedestal density of deuterium and carbon are obtained from 15 JET H-mode discharges in International Profile Database, which shown in Figs. 1 and 2. It can be seen that both parameters correlate with each other very well. Statistically, it is found that the correlation coefficient ($R^2$) between line average density and pedestal density for deuterium and carbon are 0.96 and 0.88, respectively. Thus, in this work, the following expressions are used for estimating the density of all hydrogenic and impurity species:

$$n_{\mathrm{ped,hyd}} = 0.76 n_{\mathrm{l,hyd}}$$

$$n_{\mathrm{ped,imp}} = 0.77 n_{\mathrm{l,imp}}$$

### 3. Simulation results and discussion

In this work, we have studied the behaviors of impurity in ITER by using 1.5D BALDUR integrated predictive modeling code. The engineering parameters for these scenarios are shown in table 1.

**Table 1.** The physical parameters

| Parameter | Value | Unit |
|---|---|---|
| Major radius (R) | 6.2 | m. |
| Minor radius (a) | 2.0 | m. |
| Plasma current ($I_P$) | 15 | MA |
| Magnetic field ($B_T$) | 5.3 | T |
| Elongation ( $k_{95}$) | 1.7 | - |
| Triangularity ( $\delta_{95}$) | 0.5 | - |
| Line-average density ( $\bar{n}$ ) | $10^{20}$ | $m^{-3}$ |

Deuterium, tritium, and two species of impurity are considered as plasma in all simulations, where helium is considered as one of the impurities. Another impurity can be either lithium (Li) or beryllium (Be) or carbon (C) or nitrogen (N) or oxygen (O) or neon (Ne). For each simulations, a linear combination of MMM95 anomalous transport and NCLASS neoclassical transport is used to describe both thermal and particle transports. The total auxiliary heating power used in the simulations in 40 MW. The boundary conditions are provided at the top of the pedestal. In the simulations, total run time is 2000 seconds, of which the first 100 seconds the plasma density are slowly ramped up to designated values. It is observed in all simulations that the plasma reaches stationary state quickly after the plasma density reaches the designated values. In the stationary state, the plasma still varies with some degrees of fluctuation because of numerical errors.

It is found that the central helium density in the simulations with low atomic number tends to be higher than in that with higher atomic number. This can be seen in Fig. 1. It is also found that a simulation with a lower atomic number impurity will give higher helium and impurity density for all regions from core to pedestal area.

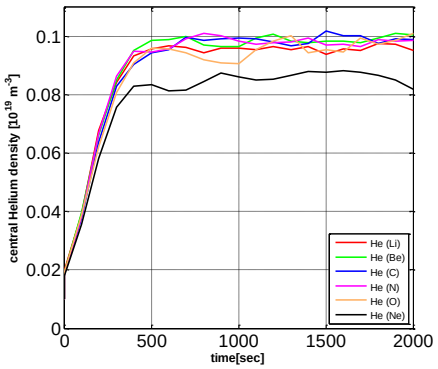


(a)

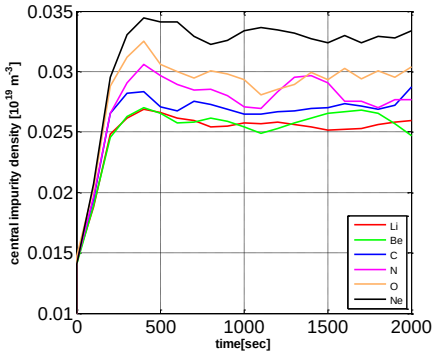


(b)

**Figure 1.** The time evolution of helium density at the plasma core in various background impurities (a). Those background impurities' density also at the plasma core (b).

# CST0007

Furthermore, the electron and ion temperature are also higher from a lower atomic number impurity, which can be seen in Fig.2.

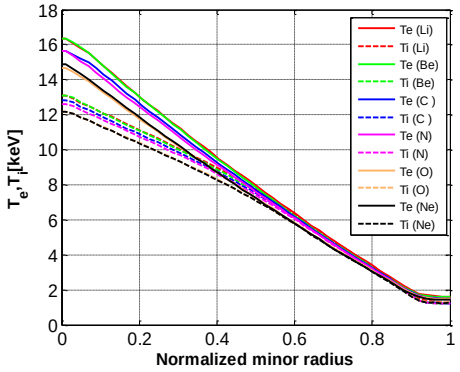


**Figure 2.** The profile of the ion and electron temperature ($T_i$ and $T_e$) at steady state during the time 2000 s is plotted as a function of the normalized minor radius.

From our simulations, this trend is also true when considering alpha power deposition, shown in Fig.3. This could be due to lower radiation loss of low atomic number impurity when comparing with higher atomic number impurity. Moreover, the decrease of impurity with the higher mass is as expected due to the increase of impurity diffusivity ($D_z$). Fig. 4 shows the profiles of average impurity diffusivity (DZ) at steady state during the time 2000 s. It is found that the average impurity diffusivity becomes larger when using impurity of higher atomic number. It can be seen that for, the kinetic ballooning term (KB) is the largest contribution in the center of the plasma, the ITG term (ITG) provides the largest contribution in the region close to the center and the resistive ballooning contribution term (RB) provides the largest contribution near the edge of the plasma. It is also found the radial profiles of the KB term are similar in all impurity scenarios. The RB profiles in different impurity scenarios are similar too except for Ne case, in which the RB term provides larger contribution near the edge and decreases dramatically at the edge of plasma. It is found that the simulation with higher mass of impurity will have higher profile of ITG term.

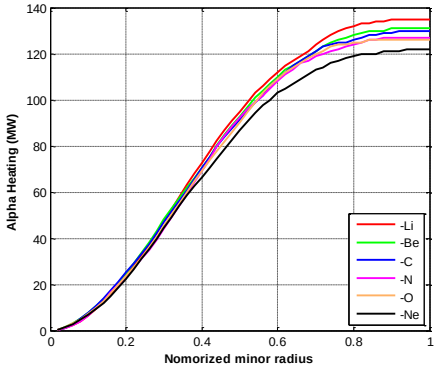


(a)

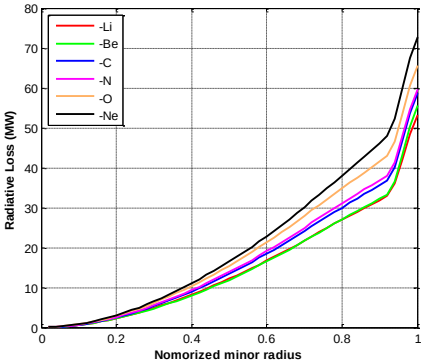


(b)

**Figure3.** The profile of alpha heating deposition (a) and radiated power deposition (b) are plotted as function the normalized radius at the time steady state 2000s.

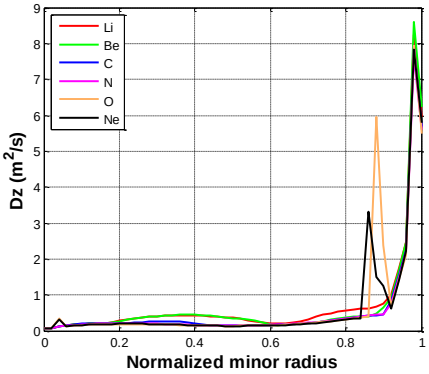


(a)

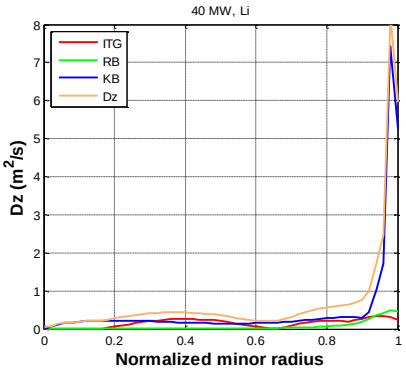


(b)

**Figure 4.** Radial profile of impurity diffusivity ($D_z$) (a) and contributing terms of impurity diffusivity (b) as function the normalized radius at the time steady state 2000s.

## 4. Conclusion

It is found that the impurity density rises to its steady-state values in all scenarios. The helium density and temperature in a steady state decrease as the atomic number of impurity increases. On the other hand, the radiation loss and impurity transport increase as the atomic number of impurity increases. Moreover, it is also found that the kinetic-ballooning term (KB) provides the largest contribution in the center of the

plasma, the ITG term (ITG) provides the largest contribution in the region between the center and the resistive ballooning contribution term (RB) provides the largest contribution near the edge of the plasma in all scenarios.

### 5. Acknowledgement

This work was supported by the Higher Education Research Promotion and National Research University Project of Thailand, Office of the Higher Education Commision"

### 6. References

[1] R P Doerner, M J Baldwin and K Schmid, Physica Scripta, Volume 2004, T111
[2] K Ohya, Physica Scripta, Volume 2006, T124
[3] R.P. Drake, J. Nuclear Energy C, 1963
[4] L. Daniel, Plasma Physics. Princeton University, 2012
[5] J. Schweinzer et al., Nuclear Fusion, 2011, 51, 113003.
[6 ] M.N.A. Beurskens et al., Nuclear Fusion, 2008, 48, 095004.
[7] W. Buangam et al., 41st EPS Conference on Plasma Physic, P5.011
[8] Z. Yong-Zhen et al., Chin. Phys. B, 2009, 18, 5406.
[9] C E. Singer et al., Comput. Phys. Commun., 1988, 49, 275-398
[10] T. Onjun et al., Nuclear Fusion, 2009, 49, 075003.
[11] D. Hannum et al., Phys. Plasmas, 2001, 8, 964-974.
[12] G. Bateman et al., Phys. Plasmas, 1998, 5, 1793-99.
[13 ] W A. Houlgerg et al., P Phys. Plasmas, 1997, 4, 3231.